NSG-7092

C S S A

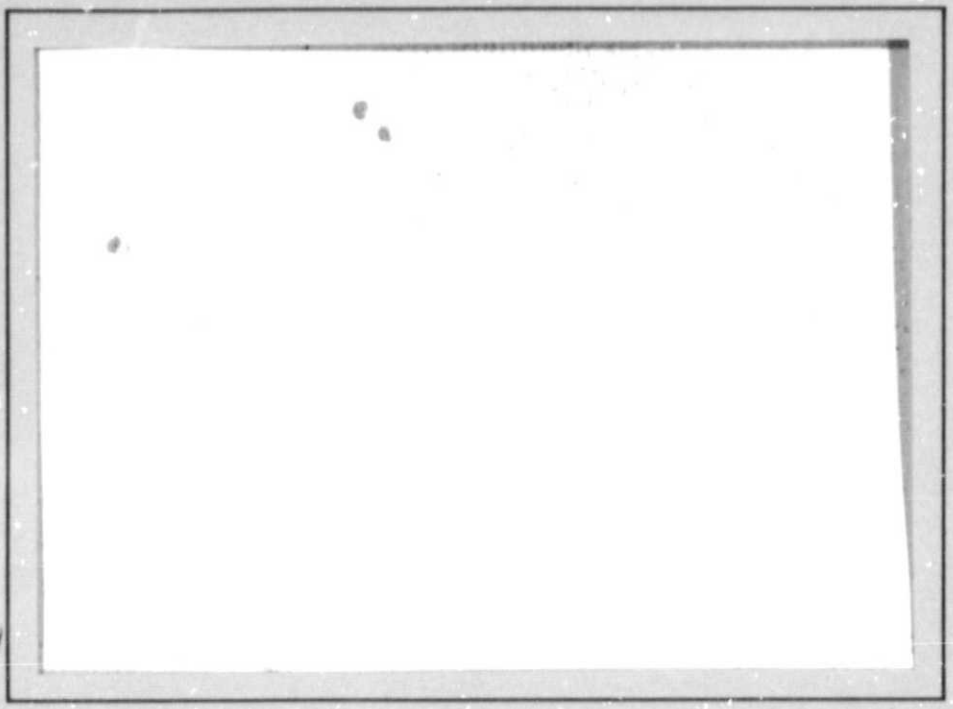

CENTER FOR SPACE SCIENCE AND ASTROPHYSICS
STANFORD UNIVERSITY
Stanford, California

DIRECTIVITY OF BREMSSTRAHLUNG RADIATION FROM RELATIVISTIC BEAMS AND THE GAMMA-RAYS FROM SOLAR FLARES

by

Vahé Petrosian[1]

CSSA-ASTRO 85-12
February 1985

[1]Also Department of Applied Physics, Stanford University

National Aeronautics and Space Administration grant NSG-7092
and
National Science Foundation grant ATM 8320439

ABSTRACT

It has been observed that flares with greater than 10 Mev gamma-ray emission are concentrated around the solar limb with a dispersion of 10 to 20 degrees. It is shown that the bremsstrahlung by relativistic electrons is responsible for such gamma-rays and that the expected relativistic beaming cannot explain this dispersion. It is argued that this dispersion is predominately a reflection of the pitch angle distribution of the electrons. Then it is shown that this requires a small variation of the magnetic field from the point where the electrons are injected to the photosphere and a nearly isotropic (in the downward direction) pitch angle distribution at the injection. The influence of other effects on the observed distribution is also briefly discussed.

I. INTRODUCTION

The gamma-ray detectors (Chupp et al 1981) on board the Solar Maximum Mission (SMM) have observed gamma-rays of up to 30 Mev from a few solar flares. The bulk of the gamma-rays (from about one to seven Mev) are produced by energetic protons (Ramaty et al 1983). The residual continuum at these and higher (10 to 30 Mev) energies must be generated by some other processes. A recent analysis of all flares with detectable signals at photon energies greater than 10 Mev by Rieger et al (1984) shows a strong concentration of bursts toward the solar limb. The histogram in figure (1) summarizes this result, where we have included four additional events from a more recent analysis (Forrest et al 1984).

This distribution is a reflection of not only the directivity of the emission but also the intrinsic distribution of the flux (or the luminosity function) at energies greater than 10 Mev. Furthermore, because the sample is chosen from a larger sample that is limited to flares with fluxes greater than certain threshold value at energies of about 300 keV, the directivity of emission and the luminosity function at this lower energy is also a contributing factor. We shall first ignore the effects of the directivity at 300 keV (which is expected and has been observed to be smaller than that at 10 Mev, Vestrand et al 1984) and the luminosity functions. We shall return to these effects at the end of the paper. Then according to the above histogram, the primary factor, namely the emission process, must be highly directional. The best candidate for this process is Coulomb bremsstrahlung by non-thermal electrons (contribution from decay of pion apparently is negligible, Ramaty et al 1983), which are known to be

responsible for production of hard x-rays. Then, the observed photons are produced by electrons of energy greater than 10 Mev Lorentz factor $\gamma > 20$) so that the relativistic beaming is very strong.

The directivity of bremsstrahlung radiation in connection with solar flares have been discussed by various authors (Elwert and Haug 1971, Brown 1972, Petrosian 1973). These studies were limited to photon energies below one Mev and ignored the curvature and convergence of the magnetic field lines, and the dispersion in pitch angle of the electron beams was treated in an approximate manner. It was clear, however, that the bremsstrahlung directivity is already significant at energies greater than a few tens of keV and increases rapidly toward higher energies.

More recent work (Leach and Petrosian 1982 and 1983, hereafter referred to as LPI and LPII), where the effects of the curvature and convergence of field lines and the diffusion in pitch angle of electrons by the elastic Coulomb collision are included, shows that the low energy x-rays will not be highly directional (cf. also Leach 1984). This is because for the non-relativistic electrons, which are responsible for hard x-rays, the energy loss rate and the diffusion rate in pitch angle are comparable so that even electrons with initial pitch angle equal to zero acquire a large mean pitch angle before they have lost a substantial fraction of their energy. In addition, the x-rays emitted by the lower energy electrons with their shorter mean free paths may come from the top as well as the lower portions of curved flare loops.

Such isotropization of electron distribution and the consequent loss of directionality of the emitted photons becomes less and less pronounced at higher and higher energies because i) the diffusion rate in pitch angle

of electrons becomes smaller than the energy loss rate at higher energies, and ii) higher energy electrons, because of their longer mean free paths, penetrate deeper into chromospheric (or photospheric) layers where the magnetic field is presumably vertical and constant over the short radiating path. We will, therefore, first consider the expected bremsstrahlung radiation from relativistic electrons injected in a uniform magnetic field region (§ II). Then, in § III, we discuss the implication of the observation for the distribution of the accelerated electrons and the parameters of the flare plasma. The effects of other characteristics on the distribution are discussed in §IV and a summary is presented in § V.

II. BREMSSTRAHLUNG RADIATION FROM RELATIVISTIC PARTICLES

As is well known, the bremsstrahlung radiation from relativistic particles is highly directional and is limited to within an angle $\theta \approx 1/\gamma$ of the direction of the emitting electrons. The cross section is a complicated function of photon energy k (which we will express in units of electron rest mass energy), electron energy , and the angle θ (see e.g. Koch and Motz 1959), but at small angles the angular dependence has the simple form $(1 + \theta^2\gamma^2)^{-2}$. At larger angles ($\theta$ order of unity) the cross section flattens out but at a level of γ^{-4} below that of small angles. For the expected steep electron energy spectra, gamma-rays of energy k are emitted mainly by electrons of energy $\gamma - 1$ slightly larger than k. Consequently, the photon distribution is also expected to be of the form $(1 + k^2\,\theta^2)^{-2}$. As shown in figure 1, this form is much narrower than the observed distribution of the gamma-ray flares, indicating that the observed distribution is a reflection of the pitch angle distribution of the electrons (and perhaps other factors), and that to first order we can approximate the cross section by a delta function. For

relativistic electrons of pitch angle α (or $\mu = \cos\alpha$) with respect to the magnetic field in a hydrogen plasma, this approximation gives (see eq. 3BS(6) of Koch and Motz 1959)

$$d^2\sigma(k,\theta) = (32\pi r_o^2\alpha_F/3)g(k,\gamma)\delta(\cos\theta-\mu)d\cos\theta dk/k \ ,$$
$$g(k,\gamma) = [1 + k/\gamma + (3/4)(k/\gamma)^2]\ln[2\gamma(\gamma- k)/ke^{1/2}] \ , \qquad (1)$$

where θ now is the angle between photon momentum and magnetic field, α_F is the fine structure constant and $r_o = 2.8 \times 10^{-13}$ cm is the classical radius of the electron. Note that this equation is valid over a limited range of $\gamma/k \gtrsim 1$. At large values of γ/k one must use the screened form of the cross section, equation 3BS(6) of Koch and Motz. This however, alters only the logarithmic term and will not be important in our analysis.

Now if $F(\gamma,\mu,s)$ is the distribution of the electrons so that $Fd\gamma d\mu ds$ is the flux (electrons/sec, i.e. flux integrated over the cross section of the magnetic tube) in the energy range $d\gamma$, pitch angle cosine range $d\mu$ and the length interval ds along the field lines, then the flux of photons $J(k,\theta)dkd\cos\theta$ (photon/sec) is

$$J(k,\theta) = (32\pi r_o^2\alpha_F/3k)\int_{1+k}^{\infty} g(\gamma,k)d\gamma \int_o^{\infty} F(\gamma,\cos\theta,s)n(s)ds \ , \qquad (2)$$

where n(s) is the density of the ambient hydrogen atoms or protons. Following LPI, we define a dimensionless column depth τ so that this can be written as

$$J(k,\theta) = (8\alpha_F/3k\ln\Lambda)\int_{1+k}^{\infty} g(k,\gamma)G(\gamma,\cos\theta)d\gamma \ ,$$
$$G(\gamma,\mu) = \int_0^{\infty} F(\gamma,\mu,\tau)d\tau, \quad d\tau = 4\pi r_o^2 \ln\Lambda n(s) \ , \qquad (3)$$

which shows that the angular distribution of the gamma-rays is determined by the integrated (over the whole emitting region) pitch angle distribution of the electrons.

For a uniform and vertical field directed toward the center of the sun, the angle θ varies from π to $\pi/2$ for flares from the center to the limb of the sun. This means that the relevant range of the pitch angles is $\pi/2 < \alpha < \pi$ (or $0 < \mu < -1$). For a more realistic case of electrons injected in a closed magnetic loop, the angle θ in the right hand side of equation (3) must be replaced by a function $\xi(\theta,..)$, which depends on the shape and orientation of the loop as well as its location on the sun (cf. e.g. Petrosian 1982). For example, for a semi-circular loop of radius R located in the plane of the solar equator $\xi = \theta + s/R - \pi/2$ where s is the distance measured from the top of the loop. However, as we mentioned above (see also below), it is unlikely that any significant number of gamma-ray photons can be produced from the upper portions of the loop where such complications must be taken into account. It should be emphasized, however, that the distribution of gamma-ray flares across the solar desk tells us only about the electron distribution with pitch angles $\alpha > \pi/2$.

III. TRANSPORT OF RELATIVISTIC ELECTRONS

The kinetic equations for a steady state transport of electrons were developed in LPI and were applied to the x-ray emission from non-relativistic electrons in LPII (cf. also Leach 1984). We now extend the application of these equations into the relativistic regime. Let us first consider all of the relevant interactions of relativistic electrons injected in a cold plasma of density n and of magnetic field of strength B.

These interactions are Coulomb collisions, bremsstrahlung, synchrotron and inverse Compton. Table 1 shows the rate of energy loss and the characteristic photon energy for each process. Clearly, for production of >10 Mev photons, bremsstrahlung is the only relevant emission process because the others will require electrons of unreasonably high energies. However, the Coulomb collisions (at high n and low B) and the synchrotron radiation (at low n and high B) are the dominant energy loss mechanisms for relativistic electrons and must be taken into account. The value of the ratio

$$R = \dot{\gamma}_s/\dot{\gamma}_c = 1.3(B/100 \text{ gauss})^2(\gamma/20)^2(20/\ln\Lambda)(10^{10}\text{cm}^{-3}/n)(1-\mu^2) \qquad (4)$$

determines which of these processes will be the dominant loss process. For ~10 Mev electrons at typical coronal values of B and n, $R_{cor} \gtrsim 1$, but at photospheric values ($n \gtrsim 10^{16}\text{cm}^{-3}$, B = 1000 gauss) $R_{phot} \lesssim 10^{-4}$.

The inverse Compton process can be ignored even as a loss process because, for normal solar soft photon density $\mathcal{E}_\gamma = L_\odot/4\pi R_\odot^2 c = 2\ \text{erg/cm}^{-3}$ it is negligible as compared to synchrotron losses when the field strength is high, $(\dot{\gamma}_s/\dot{\gamma}_{IC}) = (B/7\text{gauss})^2$, and it clearly is negligible as compared to Coulomb losses when the plasma density n is high. The inverse Compton process could become important only if the soft photon energy density $\mathcal{E}_\gamma$ is enhanced by three or four orders of magnitudes above the normal density.

We therefore consider the effects of synchrotron and collisional losses on the distribution of relativistic electrons accelerated in a plasma of density n and field strength B. For this and especially for discussion of angular distribution of any emission (bremsstrahlung here) from such electrons, we need the changes these processes inflict on the

pitch angle of the electrons. These changes are derived in the appendix and the result presented as a rate of change of pitch angle cosine $\dot{\mu}/\mu$ in Table 1. As evident, for relativistic particles, these rates are smaller than the corresponding energy loss rates. This implies that in a uniform field such particles spiral along the field lines at a constant pitch angle till they become non-relativistic. The distance along the field traveled then is

$$s_o = \int_{\gamma}^{1} \mu c\beta d\gamma/(\dot{\gamma}_s+\dot{\gamma}_c) \simeq \mu \times 10^{14}\text{cm}(10^{10}\text{cm}^{-3}/n)\ (\gamma/\ln\Lambda)\tan^{-1}(R^{\frac{1}{2}})/R^{\frac{1}{2}}\ , \qquad (5)$$

which is much longer that the length of the coronal portion of the loop (with typical size of 10^{10}cm, B = 100 gauss and n = 10^{10}cm^{-3}) except for electrons with nearly 90 degree pitch angles ($\mu < 10^{-4}$). This means that relativistic electrons will penetrate through a column depth of $N = \int nds \simeq 10^{24}\text{cm}^{-3}(\gamma/\ln\Lambda)$ and lose most of their energy through Coulomb collisions below the chromosphere at densities $n > 10^{16}\text{cm}^{-3}$. The yield of synchrotron and bremsstrahlung radiations will then be

$$Y_s \simeq R/3 \simeq 3 \times 10^{-5}(B/10^3\text{gauss})^2(10^{16}\text{cm}^{-3}/n)(\gamma/20)^2(20/\ln\Lambda)(1-\mu^2)$$
$$Y_b \simeq 5 \times 10^{-4}(\gamma/\ln\Lambda)(\ln\gamma/3) \qquad (6)$$

which are larger than the hard x-ray yield of about 10^{-5} (cf. e.g. Petrosian 1973) of non-relativistic electrons. The collisional loss time is of order of a millisecond, which is an order of magnitude shorter than the time for traversing a loop of length 10^{10} cm and is much shorter than the duration of a flare (~10 sec). This means that the acceleration of relativistic electrons (like that of the x-ray producing non-relativistic ones) must continue throughout the duration of the gamma-ray bursts.

If the accelerated electrons are injected in the corona at the top of a loop, they will encounter converging field lines and their pitch angles will change according to the adiabatic invariance relation $(1 - \mu^2)/B$ = constant. Then electrons with pitch angle in the range $\pi/2 > \alpha > \sin^{-1}(B_o/B_{tr})^{\frac{1}{2}}$ will be trapped above the transition region, where B_o and B_{tr} are the strengths of the field at the top of the loop and at the transition region, respectively.

Electrons with initial pitch angle smaller than $\sin^{-1}(B_o/B_{tr})^{\frac{1}{2}}$ will penetrate below the chromosphere, where the density scale height is much smaller than the magnetic field variation scale and radiate as in the uniform field case described above. The trapped electrons, on the other hand, will bounce back and forth till they have lost most of their energy (and have acquired non-relativistic energies) via synchrotron radiation (if $R > 1$) or Coulomb collisions (if $R < 1$). This process will last for a period of

$$t_o \simeq s_o/c = 3 \times 10^3 s(10^{10} cm^{-3}/n)(\gamma/\ln\Lambda)\tan^{-1}(R^{\frac{1}{2}})/R^{\frac{1}{2}} \qquad (7)$$

with synchrotron and bremsstrahlung yields of the order of

$$Y_s = 1 - \tan^{-1}(R^{\frac{1}{2}})/R^{\frac{1}{2}} = \begin{cases} R - 3R^2/5 + \ldots & R << 1, \\ 1 - \pi/2R^{\frac{1}{2}} + \ldots & R >> 1, \end{cases}$$

$$Y_b \simeq 5 \times 10^{-4}(\gamma/\ln\Lambda)(\ln\gamma/3)[\ln(1 + R)/R] \qquad (8)$$

This is different than the situation for non-relativistic (x-ray producing) electrons whose pitch angle changes on a time scale comparable to their energy loss time scale. This allows them to penetrate below the transition region and lose energy more quickly and increase their bremsstrahlung yield relative to their synchrotron yield.

The long life time and the low bremsstrahlung yield of the relativistic electrons dictates against a trap model unless the density in the coronal part of the loop is $>10^{12}$cm or R > 100 (e.g. $n = 10^{10}$cm , B > 1000 gauss). The first condition seems unlikely and the second one implies even a lower bremsstrahlung yield ($Y_s \sim 1$, $Y_b < 10^{-5}$). This would mean a total gamma-ray flux that is 10^5 times smaller than the total microwave and submillimeter fluxes which is contrary to observations. We, therefore, conclude that the fraction of relativistic electrons with initial pitch angles $\alpha > \sin^{-1}(B_o/B_{tr})^{\frac{1}{2}}$ must be small. This is satisfied if either the field is nearly uniform ($B_o \approx B_{tr}$) and/or the accelerated electrons (injected at the top of the loop) have small pitch angles.

For the purpose of illustration, let us assume that the injected pitch angle distribution is gaussian $F_o(\gamma,\mu) \propto \exp\{-(1-\mu^2)/\alpha_o^2\}$. Then the above discussion implies that the cases with $\alpha_o^2 >> B_o/B_{tr}$ can be ruled out because they will give too many trapped electrons.

If $\alpha_o^2 << B_o/B_{tr}$, which means a highly beamed distribution of injected electrons, then very few electrons are trapped. However, in this case, even below the transition region the electrons will be predominantly beamed downward and most of their bremsstrahlung radiation will be directed into the photosphere and absorbed there (as the albedo of the photosphere for >10 Mev photons is negligible).

The analytic expression derived in LPI are applicable in this case. As there is negligible interaction above the transition region, the pitch angle distribution at the transition region will be a broader gaussian $F_{tr}(\gamma,\mu) \propto \exp\{-(1-\mu^2)B_o/\alpha_o^2 B_{tr}\}$ than the injected one (cf. LPI eq.

7). Below the transition region the field is uniform, the density is high (so that R << 1 and synchrotron losses are negligible), and the small pitch angle solution in LPI can be easily extended to give (cf. equation A.9 in the Appendix)

$$F(\gamma,\mu,\tau) = 2F_o(\gamma+\tau)\exp\{-\alpha^2/(\alpha_o^2+\zeta)\}/(\alpha_o^2+\zeta), \quad \zeta = \gamma^{-1}\tau/(\gamma+\tau) . \qquad (9)$$

This shows that throughout the whole loop the dispersion in the pitch angle is less than $\alpha_{tr} + 2/\gamma \lesssim \alpha_{tr}^2 + 0.1$ and that at the relevant column depth $\tau = \gamma$ the dispersion is $\alpha_{tr}^2 + 1/\gamma \lesssim \alpha_{tr}^2 + 0.05$ (for $\gamma \gtrsim 20$). Since $\alpha_{tr}^2 << 1$ this implies that most particles will have pitch angles less than 10 degrees so that according to equation (3) most of the gamma-rays will also be directed downward. Only a fraction of order of γ^{-2} of the gamma-rays will be in the visible hemisphere, and the intensity of the burst at the limb will be at most twice that of those occurring at the disk center. This cannot produce the observed distribution of figure (1) and will reduce the bremsstrahlung yield of gamma-rays by a factor of $\gamma^{-2} < 0.002$. We can therefore rule out this highly beamed injection also.

The only remaining possibility is that $\alpha_{tr}^2 \simeq \alpha_o^2 B_o/B_{tr}$ so that at the transition region the electron distribution has become nearly isotropic in the downward direction. Below this region, because of this broad pitch angle distribution, analytic solutions are not possible (even though the field can be considered uniform and the synchrotron losses can be neglected) and a numerical treatment is necessary. However, we can estimate the amount of further dispersion in the diffusion approximation as follows. A distance Coulomb encounter produces an energy loss $\delta\gamma << 1$ and

causes a deflection $\delta\alpha = (2\delta\gamma/\gamma^2)^{\frac{1}{2}}$. Thus a total of $\gamma/\delta\gamma$ such encounters will produce a dispersion of the order of $(\delta\alpha)^2 = 2/\gamma$. For example, if at the transition region the electron distribution is isotropic (in the downward hemisphere), then without any dispersion the flares would be visible only within an angle $1/\gamma$ of the limb, which as shown by the thin solid line in figure 1 is in disagreement with the observed distribution. However, with the addition of the dispersion caused by the Coulomb collisions, there will be some particles moving upward with pitch angles between $\pi/2$ and $\pi/2 + (2/\gamma)^{\frac{1}{2}}$ so that the expected distribution will be wider (heavy solid curve in figure 1) which is similar to the observed one. We cannot be any more quantitative than this using analytic methods because, as described in the next section, the other factors mentioned in § I must be taken into account before reaching any quantitative conclusions. However, to show the validity of the above arguments, in figure 2 we show the expected directivity, at various relativistic photon energies, for isotropic injection in a uniform field obtained from the exact (Fokker-Planck) numerical treatment of the electron transport and the exact evaluation of the bremsstrahlung emission (i.e. without the approximation in equation 2). This clearly demonstrates the decrease in the dispersion with higher energies. The portion of the 10 Mev curve for $\theta > \pi/2$ is shown by the dashed line in figure 1, which clearly is wider than the thin line and has a characteristic dispersion of $\approx \gamma^{-\frac{1}{2}}$. This is not in exact agreement with observation, indicating that the effects described below may be important. A more detailed analysis of the problem with the inclusion of the non-uniform fields and synchrotron losses will be described elsewhere.

We conclude, therefore, that the observed distribution of the gamma-ray flares indicates that the pitch angle distribution of the electrons will be nearly isotropic in the downward direction and that the magnetic field convergence from the acceleration region (presumably in the corona) to the transition region is small.

IV. THE INFLUENCE OF OTHER FACTORS

Our discussion so far has been limited to the comparison of the directivity of the bremsstrahlung radiation, which we define as

$$D(k,\theta) = J(k,\theta)/J(k), \quad J(k) = \int J(k,\theta)d\Omega \tag{10}$$

with the observed distribution (i.e. the number of gamma-ray flares brighter than some threshold flux) across the solar disk. Such a comparison is valid only approximately for some specific and limited intrinsic distribution of fluxes J(k) (i.e. for certain luminosity functions). For a more complete analysis of this problem a knowledge of the luminosity function is also required.

In order to demonstrate this, let us assume that the luminosity function is described by a function ψ (J) such that

$$\phi(J) = \int_J^\infty \psi(x)dx \tag{11}$$

is the rate of occurrence of gamma-ray flares with flux J(k) > J. Then the observed distribution of flares as a function of the heliocentric longitude $\eta = \pi - \theta$ in a sample limited to flares with fluxes greater than J_o will be

$$n_k(\eta) = \phi[J_o/D(k,\theta)] \tag{12}$$

It is clear then that the distribution n will be proportional to $D(k,\theta)$ only if $\Phi(J) \propto J^{-1}$ or $\psi(J) \propto J^{-2}$. A large number of flares is required for an independent determination of the luminosity function. The present sample of gamma-ray flares is not sufficiently large for this task. However, at lower energies (photon energies of 25 keV), the luminosity function has the form $\Phi(X) \propto X^{-1}$ (cf. Lin 1984) so that if the same were true at 10 Mev the above comparison would be accurate.

Another effect which must be taken into account is that the observed sample of > 10 Mev gamma-ray bursts has been selected from a larger sample of bursts which are selected for having fluxes greater than certain thresholds at lower (300 keV) photon energies. The simple comparison we have made would be valid if the distribution across the solar disk of this parent sample is uniform. Any non-uniformity in this distribution will affect the analysis carried out here. In fact, this distribution is shown to be non-uniform (Vestrand et al 1984) so that in absence of other effects the observed distribution at 10 Mev should be compared with

$$n_{10\ Mev}(\eta) = n_{300\ Kev}(\eta)\phi[J_o/D(10\ Mev,\theta)] \qquad (13)$$

As mentioned earlier, the obscured $n_{300\ keV}(\eta)$ is much broader than the observed $n_{10\ Mev}(\eta)$ so that the predominant factor in (13) is the cumulative luminosity function Φ at 10 Mev.

A more complete analysis, which is beyond the scope of the present paper, will require knowledge of the directivities of bremsstrahlung at both 300 keV and at 10 Mev as well as the bivariate luminosity function ψ [J(300 keV), J(10 Mev)].

Finally, we should mention that any deviation of the magnetic field direction at large column depths ($\tau \sim 20$, $N \sim 10^{24} cm^{-2}$) from the local vertical will alter the transformatin between the angles η, θ, ξ, etc., and change the shape of the expected distribution. We should note, however, that the narrowness of the observed distribution indicates that the direction of the field lines cannot deviate strongly from the local vertical direction.

V. SUMMARY AND CONCLUSIONS

We have considered the observed distribution of flares with strong emission at photon energies of greater than 10 Mev in the framework of the model where the electrons responsible for the radiation are accelerated above the transition region and are injected in a closed magnetic loop. We have shown that:

1) Bremsstrahlung by relativistic electrons is the mechanism for production of these gamma-rays and that the production site must be deep in the photosphere where the predominant energy loss process is Coulomb collisions. The synchrotron losses can play a significant role if the magnetic field strength in the corona exceeds 1000 gauss, and the inverse Compton process could be important if the soft photon energy density in the flare region exceeds that of the quiet sun by three or four orders of magnitude.

2) The magnetic field variation from the acceleration region to the photosphere must be small to prevent trapping of the particles in the corona where they will produce mainly microwave and millimeter wavelength photon via synchrotron radiation (and very little gamma rays) for a period

much longer than the observed duration of the gamma-ray bursts.

3) The pitch angle distribution of the accelerated electrons cannot be beamed strongly along the field lines because this will result in the gamma-ray emission being directed toward the photosphere and, therefore, invisible from the Earth.

The above three conclusions can be quantitatively expressed as follows: If B_o and B_{tr} are the strengths of the field lines at the acceleration region and below the transition region, respectively, then the characteristic value of the sine of the pitch angle of the accelerated particles must be of the order of $(B_o/B_{tr})^{\frac{1}{2}}$. This requirement of nearly uniform field and/or isotropic pitch angle distribution is similar to those deduced from the consideration of the spatial structure of the microwave radiation (Petrosian 1982).

Finally, as shown in Section IV, a more quantitative conclusion in regard to the details of the model must await the determination of the distribution of the intrinsic fluxes of both gamma-ray and hard x-ray producing electrons.

APPENDIX

1) Synchrotron Losses: The radiation reaction force on a particle of mass m, charge e, energy γmc^2 and velocity $v = \beta c$ is (Panofsky and Phillips 1962).

$$\underset{\sim}{F}_r = (2e^2/3c^2)[(\gamma^4 \underset{\sim}{\beta}\cdot\ddot{\underset{\sim}{\beta}})\underset{\sim}{\beta} + \gamma^2\ddot{\underset{\sim}{\beta}}] \qquad (A.1)$$

where "." denotes time derivative. If the energy loss per gyro-period in a

magnetic field of strength B is small compared to the particle energy, then the particle will undergo helical motion with a pitch angle cosine μ and with

$$\underset{\sim}{\beta} \cdot \dot{\underset{\sim}{\beta}} = 0, \qquad \ddot{\underset{\sim}{\beta}} = -\underset{\sim}{\beta}(1-\mu^2)(2\pi\nu_b/\gamma)^2, \qquad \nu_b = 2.8\times10^6 \text{ Hz}(B/100 \text{ gauss}). \quad (A.2)$$

The rate of change of parallel and perpendicular momenta due to the radiation reaction then becomes

$$\dot{p}_{11} = -(8\pi^2 e^2\nu_b^2/3c^2)\gamma^2\beta_\perp^2\,\beta_{11}\,, \quad \dot{p}_\perp = -(8\pi e^2\nu_b^2/3c^2)(\gamma^2\beta_\perp^2 + 1)\beta_\perp\,. \qquad (A.3)$$

Transformation of these to rate of energy loss and pitch angle cosine change gives

$$(\dot{\gamma}/\gamma)_s = -(8\pi^2 r_o\nu_b^2/3c)\gamma\beta^2(1-\mu^2), \quad (\dot{\mu}/\mu)_s = (8\pi^2 r_o\nu_b^2/3c)(1-\mu^2)/\gamma \qquad (A.4)$$

These imply a continuous loss of energy and increase in the absolute value of μ. At extreme relativistic energies the change in μ is negligible while at non-relativistic energy the rate of change of energy is smaller than the rate of change of μ. In general, β_{11} = constant.

2) Coulomb collision losses. The Coulomb losses are well known and for non-relativistic regime were given in LPI. A more complete description can be found in Leach (1984), where the various logarithmic factors are explicitly evaluated. Note that the extension of LPI result into the relativistic regime gives an incorrect expression. For correct expression the quantity $(3+\gamma)/\gamma$ in the coefficient C_2 should be replaced by unity. In the present context we are interested in losses in a neutral gas.

Ignoring 20 to 40 percent contribution from helium, we can then write

$$(\dot{\gamma}/\gamma)_c = -(4\pi r_o^2 c\, n \ln\Lambda)/\beta\gamma \ , \quad (\dot{\mu}/\mu)_c = -(4\pi r_o^2 c\, n \ln\Lambda')/\beta^3\gamma^2 \qquad (A.5)$$

where $\ln\Lambda = 2\ln\Lambda' \simeq 15$ (for $\gamma \simeq 20$) and n is the neutral hydrogen density. For ionized hydrogen n would stand for the electron or proton density and $\ln\Lambda \simeq \ln\Lambda'/2 \simeq 20$. Note that unlike energy, which in the cold ambient plasma always decreases, the pitch angle can either increase or decrease so that the higher order diffusion terms must be considered. The Fokker-Planck equation described below takes this into account. As evident at relativistic energies $(\dot{\mu}/\mu)_c \ll (\dot{\gamma}/\gamma)_c$.

3) Inverse Compton Losses: The energy loss rate and the rate of change of pitch angle of relativistic electrons in a soft photon gas of energy density $\mathcal{E}_\gamma$ is similar to that of synchrotron losses with the magnetic energy density $B^2(1-\mu^2)/8\pi$ replaced by $\mathcal{E}_\gamma$ so that

$$(\dot{\gamma}/\gamma)_{I_C} \simeq -(16\pi r_o^2 c/3)(\gamma\mathcal{E}_\gamma/mc^2) \ , \quad (\dot{\mu}/\mu)_{IC} \simeq (\dot{\gamma}/\gamma)_{IC}/\gamma^2 \qquad (A.6)$$

As described in the text for the present application, the inverse Compton losses are negligible with respect to the synchrotron and Coulomb losses so that a more accurate analysis is not needed

4) The Kinetic Equation: In a strong magnetic field the gyro-radius is much smaller than the mean free path and the scale of the spatial gradient of the field, plasma density, etc. Then the independent parameters of the distribution function are the time, distance of the particle guiding center along the field, s, and the two components (parallel and perpendicular) of the momenta. It is convenient to replace

the last two by the energy $E = \gamma - 1$ and the cosine of the pitch angle, μ. The Fokker-Planck equation for the distribution function of $f(E,\mu,s,t)$ is

$$\frac{\partial f}{c\partial t} + \beta\mu\frac{\partial f}{\partial s} - \beta\frac{d\ln B}{2ds}\ (1-\mu^2)\ \frac{\partial f}{\partial \mu} = -\frac{\partial}{\partial E}\ (\dot{E}f) - \frac{\partial}{\partial \mu}\ (\dot{\mu}f) + \tfrac{1}{2}\frac{\partial^2}{\partial \mu^2}\left(\left\langle\frac{\Delta\mu\Delta\mu}{Dt}\right\rangle f\right) + \ldots\ldots \qquad (A.7)$$

In general, the higher order terms and the diffusion in energy can be neglected. The time dependence can be ignored if the acceleration and injection time scale of the electrons, as deduced from the modulation and duration of the observed emissions, is much longer than the microscopic time scale (such as energy loss time scale, etc.). Alternatively, for shorter events the integration of (A.7) over the duration of the flare is equivalent to setting $\partial f/\partial t = 0$ and having $f = f(E,\mu,s)$ represent the time integrated distribution. The result of any emission calculation should then be compared with the time-integrated fluxes.

The various possible solutions of this equation at non-relativistic energies in uniform field and when the dominant process were discussed in LPI (see also Leach 1984). As described in the text, the observations dictate a flare plasma condition whereby the Coulomb collisions will be the dominant interaction of the accelerated electron. Furthermore, these interactions will take palce over a small distance at high photospheric densities where the field can be considered uniform. In that case equation (A.7), when written in terms of the flux $F = c\beta f$, reduces to (for steady state $\partial f/\partial t = 0$)

$$\mu\frac{\partial F}{\partial \tau} = \frac{\partial}{\partial E}\left(\frac{F}{\beta^2}\right) + \frac{1}{4\beta^3\gamma^2}\ \frac{\partial}{\partial \mu}\left[(1-\mu^2)\ \frac{\partial F}{\partial \mu}\right];\quad d\tau = 4\pi r_o^2\ \ln\Lambda n ds \qquad (A.8)$$

Integrating over all depths, we find

$$\frac{\partial}{\partial}\left(\frac{G}{\beta^2}\right)+\frac{1}{4\beta^4\gamma^2}\ \frac{\partial}{\partial\mu}\ \left[(1-\mu^2)\ \frac{\partial G}{\partial\mu}\right]\ =\ \mu F_o(\mu,E)$$

$$G(\mu,E)\ =\ \int_0^{\infty}\ F(E,\mu,\tau)d\tau \qquad (A.9)$$

where $F_o(E,\mu)$ is the distribution of the accelerated electrons injected at $\tau = 0$ or $s = 0$. In the extreme relativistic case we can set $\beta = 1$ and $E = \gamma$. Even with this simplification, convenient analytic solutions are possible only for small pitch angles: $(1-\mu^2) = \alpha^2/2$, $\partial/\partial\mu = (1/\alpha)\partial/\partial\alpha$. Following LPI or Leach (1984), we find that (A.8) gives the following simple solution for an assumed gaussian, strongly beamed distribution F_o at injection.

$$F_o(\gamma,\mu)\ =\ 2F_o(\gamma)\ \exp\ \{\ -\alpha^2/\alpha_o^2\ \}/\alpha_o^2\ ,$$

$$F(\gamma,\mu,\tau)\ =\ 2F_o(\gamma+\tau)\exp\ \{-\alpha^2/(\alpha_o^2+\zeta)\}/(\alpha_o^2\ +\zeta)\ ,\quad \zeta\ =\ \gamma^{-1}\tau/(\gamma\ +\ \tau)\ . \qquad (A.10)$$

As evident, the distribution remains gaussian at all depths but with increasingly wider dispersion. However, the dispersion is always small because $\zeta < 1/\gamma$. If $\alpha_o^2 > \gamma^{-1}$, then for determination of $G(\gamma,\mu)$ it is easier to integrate (A.10) approximately than solve the differential equation (A.9). For this we write $\alpha_o^2 + \zeta = \alpha_o^2(1+\zeta/\ \alpha_o^2)$ and expand (A.9), keeping only the first order terms in ζ/α_o^2. Integration over all τ then gives

$$G(\gamma,\mu) = 2G_o(\gamma+\tau)\exp\{-\alpha^2/(\alpha_o^2+\ \overline{\zeta})\}\ /(\alpha_o^2+\ \overline{\zeta}) \qquad (A.11)$$

where

$$G_o(\gamma) = \int_{\gamma}^{\infty} F_o(\gamma')d\gamma' \quad , \quad \bar{\zeta} = \gamma^{-1} - \langle\gamma^{-1}\rangle \tag{A.12}$$

and

$$\langle \gamma^{-1}\rangle = [\int_{\gamma}^{\infty} F_o(\gamma')d\gamma'/\gamma'\,]/G_o(\gamma) \quad . \tag{A.13}$$

clearly $\bar{\zeta} \alpha 1/\gamma$ with the proportionately constant depending on the distribution $F_o(\gamma)$. For example, if $F_o(\gamma) \propto \gamma^{-n}$, then $\zeta = 1/(n\gamma)$ and $G_o(\gamma) \propto \gamma^{-n+1}$.

For $\alpha_o^2 \lesssim \gamma^{-1}$ the above procedure leads to a complicated integral which for a power law $F_o(\gamma) \propto \gamma^{-n}$ gives approximately

$$G(\gamma,\mu) \propto \gamma^{-n+1}\ [2\gamma e^{-\alpha^2\gamma}] \tag{A.14}$$

This is similar to (A.11) when γ is replaced by $\alpha_o^2 + \gamma_o^{-1}$ with $\bar{\zeta} = 1/\gamma$. The important result from this is that for relativistic electrons the pitch angle dispersion of the integrated (or mean) distribution remains small if the dispersion at injection is small.

This work was supported by the National Aeronautics and Space Administration under grant NSG 7092 and the National Science Foundation under grant ATM 8320439.

REFERENCES

Brown, J.C. 1972, Solar Phys. 26,441.

Chupp, E.L., Forrest, J.M., Ryan, M.L.. Cherry, C., Reppin, C., Kanbach, G., Rieger, E., Pinkau, K., Share, G.H.. Kinzer, R.L., Strickman, M.S., Johnson, W.N., Kurfess, J.D. 1981, Ap.J. 244, L171.

Elwert, G. and Haug, E. 1971, Solar Phys. 20, 413.

Forrest, D.J., Vestrand, W.T., Rieger, E., Cooper, J., Share, G. 1984, Bull. Amer. Ast. Soc. 16, 475.

Koch, H.W. and Motz, J.W. 1959, Phys. Rev. 31, 920.

Leach, J. 1983, Ph.D. Thesis, Stanford Univ.

Leach, J. and Petrosian, V. 1981, Ap. J. 251, 781.

Leach, J. and Petrosian, V. 1983, Ap. J. 269 715.

Lin, R.P. 1984, AIP Conf. Proc., No. 115, HIGH ENERGY TRANSIENTS IN ASTROPHYSICS, Ed. S.E. Woosley, p. 619.

Panofsky, W.K.H. and Phillips, M. 1962, CLASSICAL ELECTRICITY AND MAGNETISM, 2nd Ed., p. 393.

Petrosian, V. 1973, Ap. J. 186, 291.

Petrosian, V. 1982, Ap. J. 255, L85.

Ramaty, R., Murphy, R.J., Kozlovsky, B., Lingenfelter, R.E. 1983, Solar Phys. 86, 395.

Rieger, E., Reppin, C., Kanbach, G., Forrest, D.J., Chupp, E.L., Share, G.H. 1984, to appear in Proc. of SMM Workshop, NASA-Goddard SFC, Greenbelt, MD.

Vestrand, W.T., Forrest, E.L., Chupp, E.L., Rieger, E., Share, G.H. 1984, Bull. Amer. Ast. Soc. 16, 475.

TABLE 1

ENERGY LOSS AND PITCH ANGLE CHARGE RATES

Process	Coulomb Collision	Synchrotron	Inverse Compton	Bremsstrahlung
Energy Loss Rate $(-\dot{\gamma}/\gamma)$, s^{-1}	$3\times10^{-4}(20/\gamma)(\ln\Lambda/20)n_{10}$*	$10^{-4}(\gamma/20)(1-\mu^2)B_2^{2}$**	$2.0\times10^{-6}(\gamma/20)$	$2.5\times10^{-7}(\ln\gamma/3)n_{10}$
Pitch Angle Charge Rate $(\dot{\mu}/\mu)$, s^{-1}	$7.5\times10^{-6}(20/\gamma)^2(\ln\Lambda/20)n_{10}$	$5\times10^{-7}(20/\gamma)(1-\mu^2)B_2^{2}$	$5\times10^{-9}(20/\gamma)$	—
Characteristic Photon Energy $h\nu_c$/keV	0	$1.6\times10^{-7}(\gamma/20)^2B_2$	$0.2(\gamma/20)^2$	$\lesssim10^{4}(\gamma/20)$

* $n_{10} = (n/10^{10}\,cm^{-3})$

** $B_2 = (B/100\ gauss)$

FIGURE CAPTIONS

Figure 1. The histogram shows the observed distribution of the flares with gamma-ray emission at >10 Mev across the solar disk; $\theta = \pi/2 - \eta$ where η is the heliocentric longitude ($\eta = 0$ at the disk center, $\eta = \pi/2$ at the limb).

The lower thin curve shows the approximate behavior of the bremsstrahlung cross section at relativistic energies with the small angle from $(1+ \theta^2 k^2)^{-2}$ joined smoothly to the predominant term of the large angle form, $k^{-4}\sin^2\theta/16(1-\cos\theta)^2$; $k = 20$ (10 Mev) and θ is the angle between the electron and photon momenta. This curve can also be representing the variation of the flare brightness across the solar disk for bremsstrahlung from electrons with horizontal component of momenta.

The heavy solid line is a gaussian fit with a dispersion in angle of $\sim k^{-\frac{1}{2}}$ with $k = 20$.

The dashed line is the calculated (numerical Fokker-Planck) variation of the gamma-ray flux across the solar disk at 10 Mev (from figure 2). The angular dispersion is $\sim k^{-\frac{1}{2}}$ but the form is approximately exponential. The additional dispersion could come from other factors discussed in § IV.

Figure 2. Directivity of hard x-ray and gamma-rays from exact numerical relations from a uniform loop with isotropic (downward direction) electron injection (cf. LPII for more detail) at three different values of photon energy k. θ is the angle between the photon momentum vector and the downward vertical. Heliocentric longitude $\eta = \pi - \theta$.

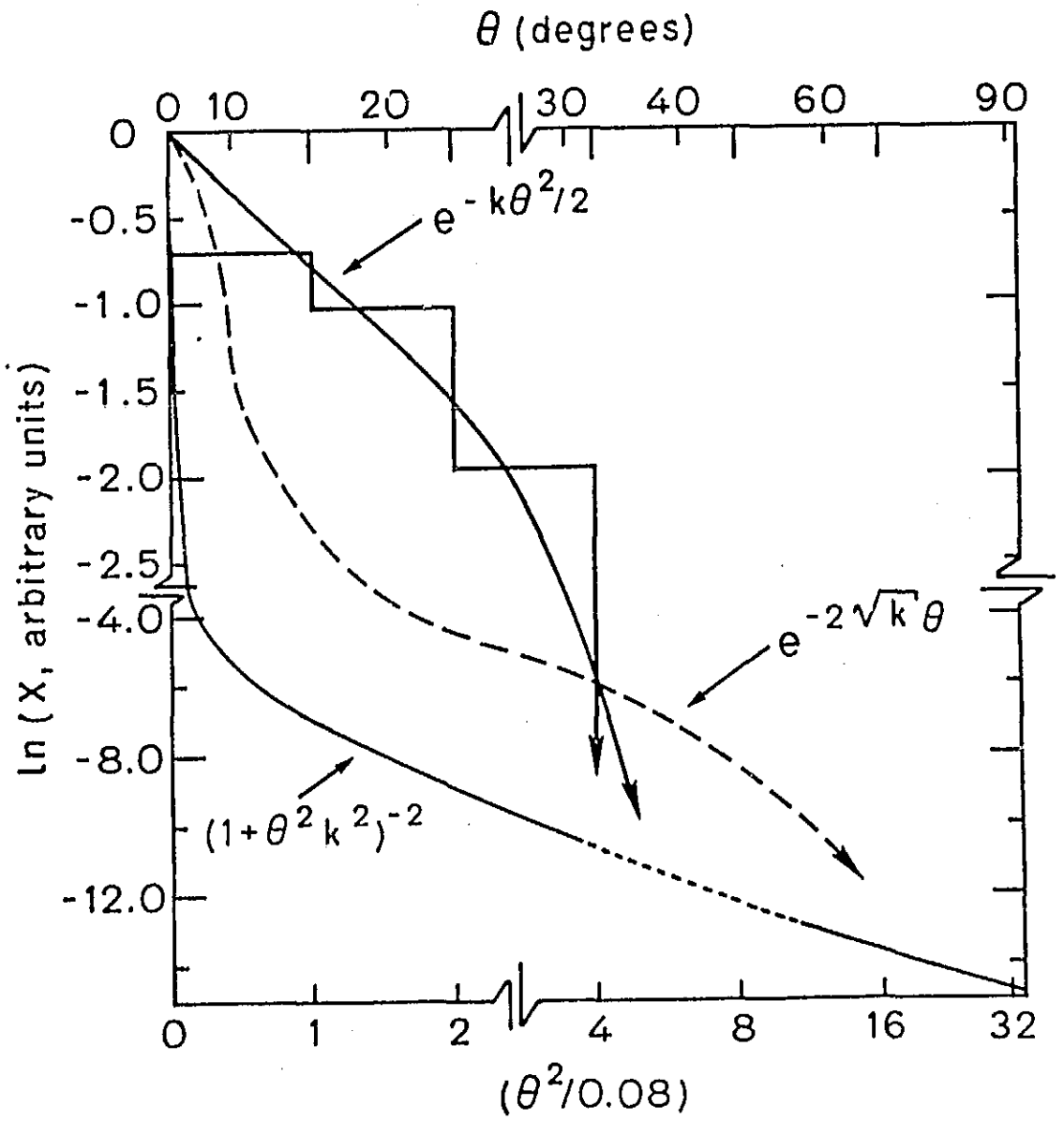
θ (degrees)
0 10 20 30 40 60 90
0
-0.5
-1.0
-1.5
-2.0
-2.5
-4.0
-8.0
-12.0
ln (X, arbitrary units)
e - kθ²/2
e -2√k θ
(1+θ²k²)-2
0 1 2 4 8 16 32
(θ²/0.08)

Figure 1

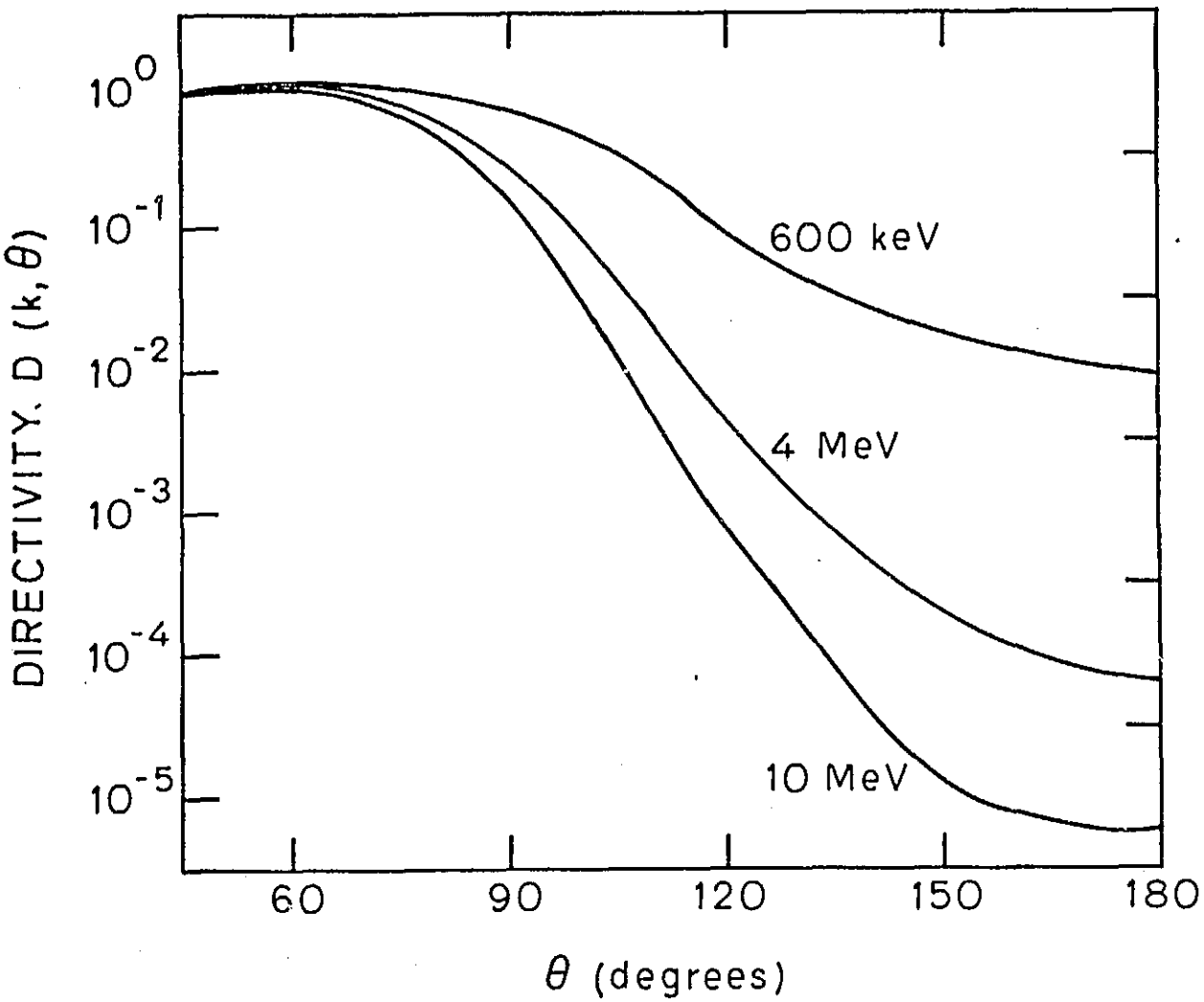
DIRECTIVITY, D (k, θ)
10^0
10^-1
10^-2
10^-3
10^-4
10^-5
600 keV
4 MeV
10 MeV
60
90
120
150
180
θ (degrees)

Figure 2